A stochastic Galerkin method for the Boltzmann equation with uncertainty*

Jingwei Hu† and Shi Jin‡

May 2, 2015

Abstract

We develop a stochastic Galerkin method for the Boltzmann equation with uncertainty. The method is based on the generalized polynomial chaos (gPC) approximation in the stochastic Galerkin framework, and can handle random inputs from collision kernel, initial data or boundary data. We show that a simple singular value decomposition of gPC related coefficients combined with the fast Fourier-spectral method (in velocity space) allows one to compute the high-dimensional collision operator very efficiently. Several numerical examples are presented to illustrate the validity of the proposed scheme.

Key words. Uncertainty quantification, the Boltzmann equation, random input, generalized polynomial chaos, stochastic Galerkin method, singular value decomposition, fast spectral method.

AMS subject classifications.

1 Introduction

Kinetic theory is an indispensable tool to describe the non-equilibrium dynamics of a gas or system comprised of a large number of particles, primarily through applications of the Boltzmann equation [4]. When the well-known fluid mechanics laws of Navier-Stokes and Fourier become inadequate to represent the system, this equation can provide reliable information at the mesoscopic level, and is widely used in the fields such as rarefied gas dynamics, astronautical engineering, etc.

While research studies on mathematical theory [7, 6, 25] and numerical approximation [5, 8] of the Boltzmann equation are extensive and still ongoing, they almost exclusively concern the deterministic problem. To authors' best knowledge, no research has been conducted to evaluate the impact of random inputs to the equation. There are, however, many sources that can bring this kind of uncertainties. For example, one of the key terms in the Boltzmann equation is the collision kernel (or cross section) which characterizes the law of interaction between particles.

*This work was partially supported by the NSF grant RNMS-1107291 (KI-Net).

†Department of Mathematics, Purdue University, West Lafayette, IN 47907, USA (hu342@purdue.edu). This author's research was also supported by a startup grant from Purdue University.

‡Department of Mathematics, University of Wisconsin-Madison, Madison, WI 53706, USA; Department of Mathematics, Institute of Natural Sciences, MOE-LSEC and SHL-MAC, Shanghai Jiao Tong University, Shanghai 200240, China (jin@math.wisc.edu). This author's research was also supported by NSF grant 1114546 and NSFC grant 91330203.

Ideally, it should be computed from the intermolecular potential using the scattering theory [14]. In practice, for simplicity, phenomenological collision kernels are often used with the aim to reproduce viscosity and diffusion coefficients [2, 17]. Specifically, these kernels contain adjustable parameters whose values can be determined by matching with the available transport data for various gases. On the other hand, when considering time evolution of a gas in bounded domains, one needs to supplement with appropriate initial and boundary conditions. These are usually given in terms of measured values of macroscopic quantities such as density, temperature, bulk velocity, etc (e.g., shock tube and Couette flow problems). In either case, one has to rely on the experimental data which inevitably involve uncertainties due to measurement errors. Therefore, it is interesting to study the behavior of the solution to the Boltzmann equation when randomness presents in the collision kernel or initial/boundary data. Most importantly, a proper quantification of these uncertainties will allow scientists and engineers to obtain more reliable predictions for sensitivity analysis and risk managements.

This paper serves as a first attempt to conduct uncertainty quantification (UQ) for the Boltzmann equation with random inputs. We will adopt the generalized polynomial chaos (gPC) based stochastic Galerkin approximation, which has been successfully applied to many physical and engineering problems, see for instance, the overviews in [13, 27]. We also mention that the same technique was used recently to solve some linear kinetic models in the diffusive limit [16]. For the Boltzmann equation, the main difficulty lies in its high-dimensional nonlinear collision integral, whose direct evaluation would be prohibitively expensive. We will show that a simple singular value decomposition (SVD) of gPC related coefficients combined with the fast spectral method in the deterministic case [22] enables one to compute the collision operator accurately and efficiently. Specifically, we are able to reduce the computational cost from $O(N_K^2 N_\sigma^{d-1} N_{\mathbf{v}}^{2d})$ to $O(R_{\mathbf{k}} N_\sigma^{d-1} N_{\mathbf{v}}^d \log N_{\mathbf{v}})$, for some $R_{\mathbf{k}} \le N_K$, where $N_K = \binom{K+n}{K}$ is the dimension of n-variate polynomials of degree up to K, d is the dimension of velocity space (typically $d = 2$ or 3), N_σ is the number of discrete points in each angular direction, and $N_{\mathbf{v}}$ is the number of points in each velocity dimension (typically $N_\sigma \ll N_{\mathbf{v}}$). To give an idea on how much speedup is gained, note that for examples, $N_K = 120$ if $K = 7, n = 3$, and $N_K = 792$ if $K = 7, n = 5$.

The rest of this paper is organized as follows. In the next section, we introduce the Boltzmann equation with random inputs and formulate the UQ problem systematically. Section 3 describes in detail the gPC based stochastic Galerkin scheme, where the fast algorithm for the collision operator as well as the time/spatial discretization are discussed. We also provide a spectral accuracy analysis of the gPC-Galerkin approximation in the random space for smooth solutions of the spatially homogeneous problem. Extensive numerical examples are presented in section 4 to illustrate the validity of the proposed scheme. Finally some conclusions are given in section 5.

2 The Boltzmann equation with random inputs

Our starting point is the following (dimensionless) deterministic Boltzmann equation [4, 25], which is the central model in kinetic theory and describes the time evolution of a rarefied gas:

$$\frac{\partial f}{\partial t} + \mathbf{v} \cdot \nabla_{\mathbf{x}} f = \frac{1}{\mathrm{Kn}} \mathcal{Q}(f, f), \quad t > 0,\ \mathbf{x}, \mathbf{v} \in \mathbb{R}^d,\ d = 2 \text{ or } 3, \tag{2.1}$$

where $f = f(t, \mathbf{x}, \mathbf{v})$ is the phase space distribution function of particles at time t, position $\mathbf{x}$, and velocity $\mathbf{v}$. Kn is the Knudsen number defined as the ratio of mean free path and typical length scale of the problem. $\mathcal{Q}(f, f)$ is the nonlinear (quadratic) Boltzmann collision operator modeling the binary interactions between particles (since $\mathcal{Q}$ acts only in the velocity space, variables t and $\mathbf{x}$ are suppressed from the functions below):

$$\mathcal{Q}(f, f)(\mathbf{v}) = \int_{\mathbb{R}^d} \int_{S^{d-1}} B(\mathbf{v} - \mathbf{v}_*, \sigma) \left[f(\mathbf{v}') f(\mathbf{v}'_*) - f(\mathbf{v}) f(\mathbf{v}_*) \right] \mathrm{d}\sigma \mathrm{d}\mathbf{v}_*. \tag{2.2}$$

Here $(\mathbf{v}, \mathbf{v}_*)$ and $(\mathbf{v}', \mathbf{v}'_*)$ are the velocity pairs before and after collision, during which the momentum and energy are conserved; hence $(\mathbf{v}', \mathbf{v}'_*)$ can be represented in terms of $(\mathbf{v}, \mathbf{v}_*)$ as

$$\begin{cases} \mathbf{v}' = \dfrac{\mathbf{v} + \mathbf{v}_*}{2} + \dfrac{|\mathbf{v} - \mathbf{v}_*|}{2} \sigma, \\ \mathbf{v}'_* = \dfrac{\mathbf{v} + \mathbf{v}_*}{2} - \dfrac{|\mathbf{v} - \mathbf{v}_*|}{2} \sigma, \end{cases}$$

with the parameter σ varying in the unit sphere S^{d-1}. The collision kernel $B(\mathbf{v} - \mathbf{v}_*, \sigma)$ is a non-negative function depending only on $|\mathbf{v} - \mathbf{v}_*|$ and cosine of the deviation angle θ:

$$B(\mathbf{v} - \mathbf{v}_*, \sigma) = B(|\mathbf{v} - \mathbf{v}_*|, \cos\theta), \quad \cos\theta = \frac{\sigma \cdot (\mathbf{v} - \mathbf{v}_*)}{|\mathbf{v} - \mathbf{v}_*|}.$$

The specific form of B is determined from the intermolecular potential via the scattering theory. For numerical purpose, a commonly used model is the *variable hard-sphere* (VHS) model introduced by Bird [2]:

$$B(|\mathbf{v} - \mathbf{v}_*|, \cos\theta) = b_\lambda |\mathbf{v} - \mathbf{v}_*|^\lambda, \quad -d < \lambda \leq 1, \tag{2.3}$$

where b_λ is a constant, $\lambda > 0$ corresponds to the hard potentials, and $\lambda < 0$ to the soft potentials.

The collision operator (2.2) conserves mass, momentum, and energy:

$$\int_{\mathbb{R}^d} \mathcal{Q}(f, f) \, \mathrm{d}\mathbf{v} = \int_{\mathbb{R}^d} \mathcal{Q}(f, f) \mathbf{v} \, \mathrm{d}\mathbf{v} = \int_{\mathbb{R}^d} \mathcal{Q}(f, f) |\mathbf{v}|^2 \, \mathrm{d}\mathbf{v} = 0.$$

Moreover, it satisfies the celebrated Boltzmann's H-theorem:

$$-\int_{\mathbb{R}^d} \mathcal{Q}(f, f) \ln f \, \mathrm{d}\mathbf{v} \geq 0,$$

which implies that the entropy is always increasing, and reaches its maximum if and only if f attains the local equilibrium:

$$\mathcal{M}(\mathbf{v})_{(\rho, \mathbf{u}, T)} = \frac{\rho}{(2\pi T)^{d/2}} e^{-\frac{(\mathbf{v} - \mathbf{u})^2}{2T}},$$

where ρ, $\mathbf{u}$, T are, respectively, the density, bulk velocity, and temperature defined by

$$\rho = \int_{\mathbb{R}^d} f(\mathbf{v}) \, \mathrm{d}\mathbf{v}, \quad \mathbf{u} = \frac{1}{\rho} \int_{\mathbb{R}^d} f(\mathbf{v}) \mathbf{v} \, \mathrm{d}\mathbf{v}, \quad T = \frac{1}{d\rho} \int_{\mathbb{R}^d} f(\mathbf{v}) |\mathbf{v} - \mathbf{u}|^2 \, \mathrm{d}\mathbf{v}. \tag{2.4}$$

When a Cauchy problem is considered, the equation (2.1) needs to be supplemented with an initial condition:

$$f(0, \mathbf{x}, \mathbf{v}) = f^0(\mathbf{x}, \mathbf{v}).$$

If we further consider a bounded spatial domain $\mathbf{x} \in \Omega \subset \mathbb{R}^d$, then a proper boundary condition also needs to be imposed. A widely used one for the Boltzmann equation is the so-called *Maxwell boundary condition*: for any boundary point $\mathbf{x} \in \partial\Omega$, let $n(\mathbf{x})$ be the unit normal vector to the boundary, pointed to the gas, then the in-flow boundary condition is specified as

$$f(t, \mathbf{x}, \mathbf{v}) = g(t, \mathbf{x}, \mathbf{v}), \quad (\mathbf{v} - \mathbf{u}_w) \cdot n > 0,$$

and

$$\begin{aligned} g(t, \mathbf{x}, \mathbf{v}) :=& (1-\alpha) f(t, \mathbf{x}, \mathbf{v} - 2[(\mathbf{v} - \mathbf{u}_w) \cdot n] n) \\ &+ \frac{\alpha}{(2\pi)^{\frac{d-1}{2}} T_w^{\frac{d+1}{2}}} e^{-\frac{|\mathbf{v}-\mathbf{u}_w|^2}{2T_w}} \int_{(\mathbf{v}-\mathbf{u}_w)\cdot n<0} f(t, \mathbf{x}, \mathbf{v}) |(\mathbf{v} - \mathbf{u}_w) \cdot n| \, \mathrm{d}\mathbf{v}, \end{aligned} \tag{2.5}$$

where $\mathbf{u}_w = \mathbf{u}_w(t, \mathbf{x})$, $T_w = T_w(t, \mathbf{x})$ are, respectively, the velocity and temperature of the wall (boundary). The constant α ($0 \le \alpha \le 1$) is the accommodation coefficient with $\alpha = 1$ corresponding to the purely diffusive boundary, and $\alpha = 0$ the purely specular reflective boundary.

Later we will also need the asymmetric collision operator:

$$\mathcal{Q}(g, h)(\mathbf{v}) = \int_{\mathbb{R}^d} \int_{S^{d-1}} B(\mathbf{v} - \mathbf{v}_*, \sigma) \left[g(\mathbf{v}') h(\mathbf{v}_*') - g(\mathbf{v}) h(\mathbf{v}_*) \right] \mathrm{d}\sigma \mathrm{d}\mathbf{v}_*. \tag{2.6}$$

As mentioned in the introduction, for real-world problems, the collision kernel, initial data, or boundary data may contain uncertainties that propagate into the solution and affect its property substantially. To quantify these uncertainties, we formulate our problem in a stochastic manner [27] as follows:

$$\begin{cases} \dfrac{\partial f}{\partial t} + \mathbf{v} \cdot \nabla_{\mathbf{x}} f = \dfrac{1}{\mathrm{Kn}} \mathcal{Q}(f, f)(t, \mathbf{x}, \mathbf{v}, \mathbf{z}), \quad t > 0, \ \mathbf{x} \in \Omega, \ \mathbf{v} \in \mathbb{R}^d, \ \mathbf{z} \in I_{\mathbf{z}}, \\ f(0, \mathbf{x}, \mathbf{v}, \mathbf{z}) = f^0(\mathbf{x}, \mathbf{v}, \mathbf{z}), \quad \mathbf{x} \in \Omega, \ \mathbf{v} \in \mathbb{R}^d, \ \mathbf{z} \in I_{\mathbf{z}}, \\ f(t, \mathbf{x}, \mathbf{v}, \mathbf{z}) = g(t, \mathbf{x}, \mathbf{v}, \mathbf{z}), \quad t \ge 0, \ \mathbf{x} \in \partial\Omega, \ \mathbf{v} \in \mathbb{R}^d, \ \mathbf{z} \in I_{\mathbf{z}}. \end{cases} \tag{2.7}$$

Now $f = f(t, \mathbf{x}, \mathbf{v}, \mathbf{z})$ depends on an extra variable $\mathbf{z}$ — an n-dimensional random vector with support $I_{\mathbf{z}}$ characterizing the random inputs of the system. The randomness could come from

- the collision kernel, for instance, $B = b_\lambda(\mathbf{z}^B)|\mathbf{v} - \mathbf{v}_*|^\lambda$;
- the boundary data $g(t, \mathbf{x}, \mathbf{v}, \mathbf{z})$, in such a way that $\mathbf{u}_w$, T_w in (2.5) are replaced by $\mathbf{u}_w(t, \mathbf{x}, \mathbf{z}^b)$ and $T_w(t, \mathbf{x}, \mathbf{z}^b)$;
- the initial data $f^0(\mathbf{x}, \mathbf{v}, \mathbf{z})$, via initial macroscopic quantities: density $\rho^0(\mathbf{x}, \mathbf{z}^i)$, temperature $T^0(\mathbf{x}, \mathbf{z}^i)$, etc.

Therefore, $\mathbf{z}$ is a collection of random vectors $\mathbf{z}^B$, $\mathbf{z}^b$ and $\mathbf{z}^i$, summed up to dimension n, i.e., $\mathbf{z} := (\mathbf{z}^B, \mathbf{z}^b, \mathbf{z}^i) = (z_1, \ldots, z_n)$. For simplicity, we assume in this paper, the components of $\mathbf{z}$ are mutually independent random variables already obtained through some dimension reduction technique, e.g., Karhunen-Loève expansion [18], and do not pursue further the issue of random input parameterization.

3 A gPC based stochastic Galerkin method

In this section, we construct a stochastic Galerkin scheme for the problem (2.7) using gPC expansion. Specifically, we seek a solution in the following form:

$$f(t,\mathbf{x},\mathbf{v},\mathbf{z}) \approx P_K f = \sum_{|\mathbf{k}|=0}^{K} f_{\mathbf{k}}(t,\mathbf{x},\mathbf{v})\Phi_{\mathbf{k}}(\mathbf{z}), \tag{3.1}$$

$$f_{\mathbf{k}}(t,\mathbf{x},\mathbf{v}) = \int_{I_{\mathbf{z}}} f(t,\mathbf{x},\mathbf{v},\mathbf{z})\Phi_{\mathbf{k}}(\mathbf{z})\pi(\mathbf{z})\,\mathrm{d}\mathbf{z}. \tag{3.2}$$

Here $\mathbf{k}=(k_1,\ldots,k_n)$ is a multi-index with $|\mathbf{k}| = k_1+\cdots+k_n$. $\{\Phi_{\mathbf{k}}(\mathbf{z})\}$ are orthonormal gPC basis functions satisfying

$$\int_{I_{\mathbf{z}}} \Phi_{\mathbf{k}}(\mathbf{z})\Phi_{\mathbf{j}}(\mathbf{z})\pi(\mathbf{z})\,\mathrm{d}\mathbf{z} = \delta_{\mathbf{kj}}, \quad 0 \le |\mathbf{k}|, |\mathbf{j}| \le K,$$

where $\pi(\mathbf{z})$ is the probability distribution function of $\mathbf{z}$. The approximation (3.1) is optimal in space $\mathbb{P}_K^n$ (the set of all n-variate polynomials of degree up to K) in the sense that

$$\|f - P_K f\|_{L^2_\pi} = \inf_{h\in\mathbb{P}_K^n} \|f-h\|_{L^2_\pi}.$$

Inserting (3.1) into (2.7), and performing a standard Galerkin projection, we get

$$\begin{cases} \dfrac{\partial f_{\mathbf{k}}}{\partial t} + \mathbf{v}\cdot\nabla_{\mathbf{x}} f_{\mathbf{k}} = \dfrac{1}{\mathrm{Kn}} Q_{\mathbf{k}}(P_K f, P_K f)(t,\mathbf{x},\mathbf{v}), \quad t>0,\ \mathbf{x}\in\Omega,\ \mathbf{v}\in\mathbb{R}^d, \\ f_{\mathbf{k}}(0,\mathbf{x},\mathbf{v}) = f^0_{\mathbf{k}}(\mathbf{x},\mathbf{v}), \quad \mathbf{x}\in\Omega,\ \mathbf{v}\in\mathbb{R}^d, \\ f_{\mathbf{k}}(t,\mathbf{x},\mathbf{v}) = g_{\mathbf{k}}(t,\mathbf{x},\mathbf{v}), \quad t\ge 0,\ \mathbf{x}\in\partial\Omega,\ \mathbf{v}\in\mathbb{R}^d \end{cases} \tag{3.3}$$

for each $0\le|\mathbf{k}|\le K$, and

$$\begin{aligned} Q_{\mathbf{k}}(P_K f, P_K f) &:= \int_{I_{\mathbf{z}}} \mathcal{Q}(P_K f, P_K f)(t,\mathbf{x},\mathbf{v},\mathbf{z})\Phi_{\mathbf{k}}(\mathbf{z})\pi(\mathbf{z})\,\mathrm{d}\mathbf{z}, \\ f^0_{\mathbf{k}} &:= \int_{I_{\mathbf{z}}} f^0(\mathbf{x},\mathbf{v},\mathbf{z})\Phi_{\mathbf{k}}(\mathbf{z})\pi(\mathbf{z})\,\mathrm{d}\mathbf{z}, \\ g_{\mathbf{k}} &:= \int_{I_{\mathbf{z}}} g(t,\mathbf{x},\mathbf{v},\mathbf{z})\Phi_{\mathbf{k}}(\mathbf{z})\pi(\mathbf{z})\,\mathrm{d}\mathbf{z}. \end{aligned}$$

Remark 3.1 *$Q_{\mathbf{k}}$ conserves mass, momentum and energy as $\mathcal{Q}(f,f)$. However, the H-theorem no longer holds since $P_K f$ loses positivity.*

For the VHS collision kernel (2.3) with uncertainty in b_λ, $Q_{\mathbf{k}}$ can be further expanded as

$$Q_{\mathbf{k}} = \sum_{|\mathbf{i}|,|\mathbf{j}|=0}^{K} S_{\mathbf{kij}} \int_{\mathbb{R}^d}\int_{S^{d-1}} |\mathbf{v}-\mathbf{v}_*|^\lambda \left[f_{\mathbf{i}}(\mathbf{v}')f_{\mathbf{j}}(\mathbf{v}'_*) - f_{\mathbf{i}}(\mathbf{v})f_{\mathbf{j}}(\mathbf{v}_*)\right]\mathrm{d}\sigma\mathrm{d}\mathbf{v}_*, \tag{3.4}$$

with

$$S_{\mathbf{kij}} := \int_{I_{\mathbf{z}}} b_\lambda(\mathbf{z})\Phi_{\mathbf{k}}(\mathbf{z})\Phi_{\mathbf{i}}(\mathbf{z})\Phi_{\mathbf{j}}(\mathbf{z})\pi(\mathbf{z})\,\mathrm{d}\mathbf{z}.$$

For the Maxwell boundary condition (2.5) with uncertainty in T_w (assume $\mathbf{u}_w = 0$ for simplicity), $g_{\mathbf{k}}$ is given by

$$g_{\mathbf{k}} = (1-\alpha) f_{\mathbf{k}}(t, \mathbf{x}, \mathbf{v} - 2(\mathbf{v}\cdot n)n) + \alpha \sum_{|\mathbf{j}|=0}^{K} D_{\mathbf{kj}}(\mathbf{x}, \mathbf{v}) \int_{\mathbf{v}\cdot n<0} f_{\mathbf{j}}(t, \mathbf{x}, \mathbf{v}) |\mathbf{v}\cdot n| \, \mathrm{d}\mathbf{v}, \tag{3.5}$$

with

$$D_{\mathbf{kj}}(\mathbf{x}, \mathbf{v}) := \int_{I_{\mathbf{z}}} \frac{e^{-\frac{\mathbf{v}^2}{2T_w(\mathbf{x},\mathbf{z})}}}{(2\pi)^{\frac{d-1}{2}} T_w^{\frac{d+1}{2}}(\mathbf{x}, \mathbf{z})} \Phi_{\mathbf{k}}(\mathbf{z}) \Phi_{\mathbf{j}}(\mathbf{z}) \pi(\mathbf{z}) \, \mathrm{d}\mathbf{z}.$$

In (3.5), since $D_{\mathbf{kj}}$ does not depend on the solution $f_{\mathbf{k}}$, it can be precomputed accurately and stored for repeated use. Likewise, $S_{\mathbf{kij}}$ in (3.4) can also be precomputed, but even so, the evaluation of $Q_{\mathbf{k}}$ still presents a challenge. A naive, direct computation for each t and $\mathbf{x}$ would result in $O(N_K^2 N_\sigma^{d-1} N_{\mathbf{v}}^{2d})$ complexity, where $N_K = \binom{K+n}{K}$ is the dimension of $\mathbb{P}_K^n$, N_σ is the number of discrete points in each angular direction, and $N_{\mathbf{v}}$ is the number of points in each velocity dimension. This is, if not impossible, prohibitively expensive.

3.1 A fast algorithm for the collision operator

In this subsection, we leverage the existing fast spectral method for the deterministic collision operator [22] to construct a fast algorithm for (3.4). We show that with the help of the SVD, one can easily reduce the above direct cost from $O(N_K^2 N_\sigma^{d-1} N_{\mathbf{v}}^{2d})$ to $O(N_K N_\sigma^{d-1} N_{\mathbf{v}}^{d} \log N_{\mathbf{v}})$ (in practice, typically $N_\sigma \ll N_{\mathbf{v}}$ [11, 10]). This is achieved in two steps.

First, for each fixed $\mathbf{k}$, decompose the symmetric matrix $(S_{\mathbf{kij}})_{N_K \times N_K}$ as (via a truncated SVD with desired accuracy)

$$S_{\mathbf{kij}} = \sum_{r=1}^{R_{\mathbf{k}}} U_{\mathbf{i}r}^{\mathbf{k}} V_{r\mathbf{j}}^{\mathbf{k}}.$$

Substituting it into (3.4) and rearranging terms, we get

$$Q_{\mathbf{k}} = \sum_{r=1}^{R_{\mathbf{k}}} \int_{\mathbb{R}^d} \int_{S^{d-1}} |\mathbf{v} - \mathbf{v}_*|^\lambda \left[g_r^{\mathbf{k}}(\mathbf{v}') h_r^{\mathbf{k}}(\mathbf{v}_*') - g_r^{\mathbf{k}}(\mathbf{v}) h_r^{\mathbf{k}}(\mathbf{v}_*) \right] \mathrm{d}\sigma \mathrm{d}\mathbf{v}_*, \tag{3.6}$$

with

$$g_r^{\mathbf{k}}(\mathbf{v}) := \sum_{|\mathbf{i}|=0}^{K} U_{\mathbf{i}r}^{\mathbf{k}} f_{\mathbf{i}}(\mathbf{v}), \quad h_r^{\mathbf{k}}(\mathbf{v}) := \sum_{|\mathbf{i}|=0}^{K} V_{r\mathbf{i}}^{\mathbf{k}} f_{\mathbf{i}}(\mathbf{v}).$$

Hence we readily reduce the cost from $O(N_K^2 N_\sigma^{d-1} N_{\mathbf{v}}^{2d})$ to $O(R_{\mathbf{k}} N_\sigma^{d-1} N_{\mathbf{v}}^{2d})$, where $R_{\mathbf{k}} \le N_K$ is the numerical rank of matrix $(S_{\mathbf{kij}})_{N_K \times N_K}$.

Remark 3.2 *The value of $R_{\mathbf{k}}$ is closely related to the properties of $\{\Phi_{\mathbf{k}}(\mathbf{z})\}$ and $b_\lambda(\mathbf{z})$, and deserves further investigation. In our numerical examples using Legendre polynomials, we observe that for prescribed accuracy 10^{-12}, $R_{\mathbf{k}} \equiv N_K$ for $n = 1$, and $R_{\mathbf{k}} \le N_K$ for $n = 2$ (some $R_{\mathbf{k}}$ can be significantly less than N_K and results in further saving). We also mention that the tensor $S_{\mathbf{kij}}$ itself has some sparse structure owing to the orthogonality of basis and many symmetries, as discussed in [21]. In principle, one can identify its nonzero values and perform computation (3.4) only on those points. The SVD approach we used here is a simple alternative, and is feasible when N_K is not very large.*

Next, note that (3.6) can be formally written as

$$Q_{\mathbf{k}} = \sum_{r=1}^{R_{\mathbf{k}}} \mathcal{Q}(g_r^{\mathbf{k}}, h_r^{\mathbf{k}}), \tag{3.7}$$

and $\mathcal{Q}$ is the deterministic collision operator (2.6) with kernel $B = |\mathbf{v} - \mathbf{v}_*|^\lambda$. In [22], a fast Fourier-spectral method in velocity variable $\mathbf{v}$ was developed for (2.2) in the case of 2D Maxwell molecule ($\lambda = 0$) and 3D hard-sphere molecule ($\lambda = 1$). Applying this method to (3.7) with slight modification, one can further reduce the cost from $O(R_{\mathbf{k}} N_\sigma^{d-1} N_{\mathbf{v}}^{2d})$ to $O(R_{\mathbf{k}} N_\sigma^{d-1} N_{\mathbf{v}}^{d} \log N_{\mathbf{v}})$ (see appendix for a detailed description).

3.2 Time and spatial discretizations

A semi-discrete scheme for (3.3) consists of two steps:

- *Convection step:*
$$\frac{f_{\mathbf{k}}^* - f_{\mathbf{k}}^n}{\Delta t} + \mathbf{v} \cdot \nabla_{\mathbf{x}} f_{\mathbf{k}}^n = 0;$$
- *Collision step:*
$$\frac{f_{\mathbf{k}}^{n+1} - f_{\mathbf{k}}^*}{\Delta t} = \frac{1}{\mathrm{Kn}} Q_{\mathbf{k}}^*.$$

For the spatial derivative in the convection step, we employ the second-order MUSCL scheme [24]. Second-order accuracy in time can be achieved using Runge-Kutta scheme and Strang splitting.

Remark 3.3 *In this paper, we don't consider very small Knudsen number, thus an explicit scheme is used for the collision step. Developing efficient numerical schemes that work uniformly for a wide range of Kn constitutes an active research area called "asymptotic-preserving scheme" [15]. This is currently under consideration in the context of UQ.*

3.3 Computation of the moments

When solving the Boltzmann equation, besides the directly evolved density distribution function, people are also interested in its various moments such as those in (2.4). In the stochastic Galerkin method, a remaining issue is: given $f_{\mathbf{k}}$, how to obtain reasonable gPC expansion coefficients for macroscopic quantities? Inspired by [21], we proceed as follows:

- Compute $\rho_{\mathbf{k}}$, $\mathbf{m}_{\mathbf{k}}$, and $E_{\mathbf{k}}$ by direct integration
$$\rho_{\mathbf{k}} := \int_{\mathbb{R}^d} f_{\mathbf{k}} \, \mathrm{d}\mathbf{v}, \quad \mathbf{m}_{\mathbf{k}} := \int_{\mathbb{R}^d} f_{\mathbf{k}} \mathbf{v} \, \mathrm{d}\mathbf{v}, \quad E_{\mathbf{k}} := \frac{1}{2} \int_{\mathbb{R}^d} f_{\mathbf{k}} |\mathbf{v}|^2 \, \mathrm{d}\mathbf{v}.$$
- Compute $\rho_{\mathbf{k}}^{-1}$ from
$$\rho\rho^{-1} = 1 \Rightarrow \left(\sum_{|\mathbf{i}|=0}^{K} \rho_{\mathbf{i}} \Phi_{\mathbf{i}} \right) \left(\sum_{|\mathbf{j}|=0}^{K} \rho_{\mathbf{j}}^{-1} \Phi_{\mathbf{j}} \right) = 1,$$

which upon projection amounts to solving the linear system

$$\sum_{|\mathbf{j}|=0}^{K} a_{\mathbf{kj}} \rho_{\mathbf{j}}^{-1} = \delta_{\mathbf{0k}}$$

with

$$a_{\mathbf{kj}} := \sum_{|\mathbf{i}|=0}^{K} \rho_{\mathbf{i}} S'_{\mathbf{kij}}, \quad S'_{\mathbf{kij}} := \int_{I_{\mathbf{z}}} \Phi_{\mathbf{k}}(\mathbf{z}) \Phi_{\mathbf{i}}(\mathbf{z}) \Phi_{\mathbf{j}}(\mathbf{z}) \pi(\mathbf{z}) \, \mathrm{d}\mathbf{z}.$$

- Compute $\mathbf{u_k}$ and $T_{\mathbf{k}}$ via

$$u_{\mathbf{k}}^{(l)} = \sum_{|\mathbf{i}|,|\mathbf{j}|=0}^{K} m_{\mathbf{i}}^{(l)} \rho_{\mathbf{j}}^{-1} S'_{\mathbf{kij}},$$
$$T_{\mathbf{k}} = \frac{2}{d} \sum_{|\mathbf{i}|,|\mathbf{j}|=0}^{K} \left(E_{\mathbf{i}} \rho_{\mathbf{j}}^{-1} - \frac{1}{2} \sum_{l=1}^{d} u_{\mathbf{i}}^{(l)} u_{\mathbf{j}}^{(l)} \right) S'_{\mathbf{kij}},$$

  where superscripts l denote the lth component of a d-dimensional vector.

3.4 A spectral accuracy analysis

In this subsection we perform a (non-rigorous) spectral accuracy analysis for smooth solutions on the gPC Galerkin approximation (while keeps other variables continuous). For notation clarification we assume space homogeneity and suppress the spatial dependence. We also omit the Knudsen number Kn in front of the collision term.

First, if one applies directly the exact solution

$$\hat{f}(t, \mathbf{v}, \mathbf{z}) = \sum_{|\mathbf{k}|=0}^{\infty} \hat{f}_{\mathbf{k}}(t, \mathbf{v}) \Phi_{\mathbf{k}}(\mathbf{z})$$

into the Boltzmann equation (2.7) and carries out the Galerkin projection, one will get

$$\frac{\partial \hat{f}_{\mathbf{k}}}{\partial t} = Q_{\mathbf{k}}(\hat{f}, \hat{f}), \quad t > 0.$$

Define the numerical error as

$$e_{\mathbf{k}} = \hat{f}_{\mathbf{k}} - f_{\mathbf{k}}, \quad |\mathbf{k}| \le K, \qquad \mathbf{e} = (e_1, \cdots, e_{N_K})^T,$$

then one has the following equation for the error:

$$\frac{\partial e_{\mathbf{k}}}{\partial t} = Q_{\mathbf{k}}(\hat{f}, \hat{f}) - Q_{\mathbf{k}}(P_K f, P_K f). \tag{3.8}$$

We now estimate the right hand side of (3.8) for consistency error. We first state a basic property of the collision operator (see for example [3, 19]):

Lemma 3.4 *If $g, h \in L^2_{\mathbf{v}}$, the L^2 space in $\mathbf{v}$, then*

$$\|\mathcal{Q}(g, h)\|_{L^2_{\mathbf{v}}} \le C_B \|g\|_{L^2_{\mathbf{v}}} \|h\|_{L^2_{\mathbf{v}}},$$

where $C_B > 0$ only depends on the collision kernel B.

Since our B depends on $\mathbf{z}$, C_B will depend on $\mathbf{z}$. Below we assume that it has an upper bound for all $\mathbf{z}$. Furthermore, we assume the regularity of $\hat{f}$ as needed, and assume $P_K f$ bounded uniformly in K in the space needed. Then,

$$
\begin{aligned}
& \|Q_{\mathbf{k}}(\hat{f},\hat{f}) - Q_{\mathbf{k}}(P_K f, P_K f)\|_{L^2_{\mathbf{v}}}^2 \\
= & \int_{\mathbb{R}^d} \left(\int_{I_{\mathbf{z}}} [\mathcal{Q}(\hat{f},\hat{f})(t,\mathbf{v},\mathbf{z}) - \mathcal{Q}(P_K f, P_K f)(t,\mathbf{v},\mathbf{z})] \Phi_{\mathbf{k}}(\mathbf{z}) \pi(\mathbf{z})\, \mathrm{d}\mathbf{z} \right)^2 \mathrm{d}\mathbf{v} \\
= & \int_{\mathbb{R}^d} \left(\int_{I_{\mathbf{z}}} [\mathcal{Q}(\hat{f} - P_K f, \hat{f})(t,\mathbf{v},\mathbf{z}) + \mathcal{Q}(P_K f, \hat{f} - P_K f)(t,\mathbf{v},\mathbf{z})] \Phi_{\mathbf{k}}(\mathbf{z}) \pi(\mathbf{z})\, \mathrm{d}\mathbf{z} \right)^2 \mathrm{d}\mathbf{v} \\
\le & \int_{\mathbb{R}^d} \left(\int_{I_{\mathbf{z}}} [\mathcal{Q}(\hat{f} - P_K f, \hat{f})(t,\mathbf{v},\mathbf{z}) + \mathcal{Q}(P_K f, \hat{f} - P_K f)(t,\mathbf{v},\mathbf{z})]^2 \pi(\mathbf{z})\, \mathrm{d}\mathbf{z} \right) \left(\int_{I_{\mathbf{z}}} \Phi_{\mathbf{k}}^2(\mathbf{z}) \pi(\mathbf{z})\, \mathrm{d}\mathbf{z} \right) \mathrm{d}\mathbf{v} \\
= & \int_{I_{\mathbf{z}}} \int_{\mathbb{R}^d} [\mathcal{Q}(\hat{f} - P_K f, \hat{f})(t,\mathbf{v},\mathbf{z}) + \mathcal{Q}(P_K f, \hat{f} - P_K f)(t,\mathbf{v},\mathbf{z})]^2 \mathrm{d}\mathbf{v}\, \pi(\mathbf{z})\, \mathrm{d}\mathbf{z} \\
\le & 2 \int_{I_{\mathbf{z}}} \left(\|\mathcal{Q}(\hat{f} - P_K f, \hat{f})(t,\cdot,\mathbf{z})\|_{L^2_{\mathbf{v}}}^2 + \|\mathcal{Q}(P_K f, \hat{f} - P_K f)(t,\cdot,\mathbf{z})\|_{L^2_{\mathbf{v}}}^2 \right) \pi(\mathbf{z})\, \mathrm{d}\mathbf{z} \\
\le & 2C_B^2 \int_{I_{\mathbf{z}}} \left(\|\hat{f}\|_{L^2_{\mathbf{v}}}^2 \|\hat{f} - P_K f\|_{L^2_{\mathbf{v}}}^2 + \|P_K f\|_{L^2_{\mathbf{v}}}^2 \|\hat{f} - P_K f\|_{L^2_{\mathbf{v}}}^2 \right) \pi(\mathbf{z})\, \mathrm{d}\mathbf{z} \\
\le & C \int_{I_{\mathbf{z}}} \|\hat{f} - P_K f\|_{L^2_{\mathbf{v}}}^2 \pi(\mathbf{z})\, \mathrm{d}\mathbf{z}, \\
\le & C \int_{I_{\mathbf{z}}} \left(\|\hat{f} - P_K \hat{f}\|_{L^2_{\mathbf{v}}}^2 + \|P_K(\hat{f} - f)\|_{L^2_{\mathbf{v}}}^2 \right) \pi(\mathbf{z})\, \mathrm{d}\mathbf{z} \\
\le & C \left\{ \frac{1}{K^{2m}} + \|\mathbf{e}\|_{L^2_{\mathbf{v}}}^2 \right\}
\end{aligned}
$$

where in the first inequality we used Cauchy-Schwartz inequality, in the third inequality we used Lemma 3.4, in the fourth inequality we used the assumed boundedness of $\hat{f}$ and uniform boundedness of $P_K f$ in K, and in the last inequality we used the spectral accuracy of the P_K operator

$$\|\hat{f} - P_K \hat{f}\|_{L^2_{\mathbf{v}}} = O(K^{-m}) \tag{3.9}$$

where m comes from regularity assumption in the random space. $C > 0$ is a generic constant.

Now multiplying both sides of (3.8) by $e_{\mathbf{k}}$, summing over $\mathbf{k}$, and using Cauchy-Schwartz inequality on the right hand side, one can easily derive the following inequality:

$$\frac{\partial}{\partial t} \|\mathbf{e}\|_{L^2_{\mathbf{v}}} \le C \left\{ \frac{1}{K^m} + \|\mathbf{e}\|_{L^2_{\mathbf{v}}} \right\}.$$

By Gronwall's inequality one obtains

$$\|\mathbf{e}(t)\|_{L^2_{\mathbf{v}}} \le e^{Ct} \left\{ \frac{1}{K^m} + \|\mathbf{e}(0)\|_{L^2_{\mathbf{v}}} \right\}. \tag{3.10}$$

Finally,

$$\|\hat{f} - P_K f\|_{L^2_{\mathbf{v}}} \le \|P_K(\hat{f} - f)\|_{L^2_{\mathbf{v}}} + \|\hat{f} - P_K \hat{f}\|_{L^2_{\mathbf{v}}}.$$

This, together with (3.10) gives

$$\|\hat{f} - P_K f\|_{L^2_{\mathbf{v}}} \le C(t) \left\{ \frac{1}{K^m} + \|\mathbf{e}(0)\|_{L^2_{\mathbf{v}}} \right\}$$

which shows the spectral accuracy for smooth solutions.

Remark 3.5 *One can combine the spectral accuracy analysis in the random space and the spectral accuracy analysis for the collision operator established in [22] to obtain a spectral accuracy for the combined random space and velocity space. We omit the straightforward details.*

4 Numerical examples

In this section, we present several numerical examples to illustrate the validity of the proposed scheme. We will consider both spatially homogeneous and inhomogeneous problems, wherein the randomness can come from collision kernel, initial data, or boundary data. For simplicity, we will always assume the random variable $\mathbf{z}$ obeys the uniform distribution on $[-1,1]^n$ with n up to 2, thus the Legendre polynomials are used as gPC basis. Given the gPC coefficients $f_{\mathbf{k}}$ of f, the statistical information mean, variance, and standard deviation are retrieved as

$$\mathbb{E}[f] = f_{\mathbf{0}}, \quad \mathrm{Var}[f] \approx \sum_{|\mathbf{k}|=1}^{K} f_{\mathbf{k}}^2, \quad S[f] \approx \sqrt{\sum_{|\mathbf{k}|=1}^{K} f_{\mathbf{k}}^2}.$$

4.1 The spatially homogeneous BGK equation

Example 1. We first consider the homogeneous BGK equation

$$\frac{\partial f}{\partial t} = B(\mathbf{z})(\mathcal{M} - f), \quad v \in \mathbb{R}$$

with random collision kernel

$$B(\mathbf{z}) = 1 + s_1 z_1 + s_2 z_2, \quad s_1 = 0.2,\ s_2 = 0.1,$$

and deterministic initial condition

$$f^0(v) = v^2 e^{-v^2}.$$

This is a particularly simple example where the Maxwellian $\mathcal{M}$ neither depends on $\mathbf{z}$ nor changes in time. Figure 1 shows the mean and standard deviation of f obtained using gPC up to 7th degree. The fourth-order Runge-Kutta scheme is applied for time discretization. The velocity space is discretized using 64 points.

To further verify the accuracy of the scheme, we conduct the convergence analysis by comparing with the exact solution. Results are gathered in Figure 2, where we clearly observe the spectral accuracy in random space and desired accuracy in time.

4.2 The spatially homogeneous Boltzmann equation

We now consider the homogeneous Boltzmann equation. In this and the rest of examples, we always assume 2D Maxwell molecules, i.e., $\mathbf{v} \in \mathbb{R}^2$ and $\lambda = 0$ in (2.3). Extension to 3D is straightforward.

4.2.1 Random collision kernel

Example 2. Assume the collision kernel

$$B(z) = 1 + sz, \quad s = 0.2,$$

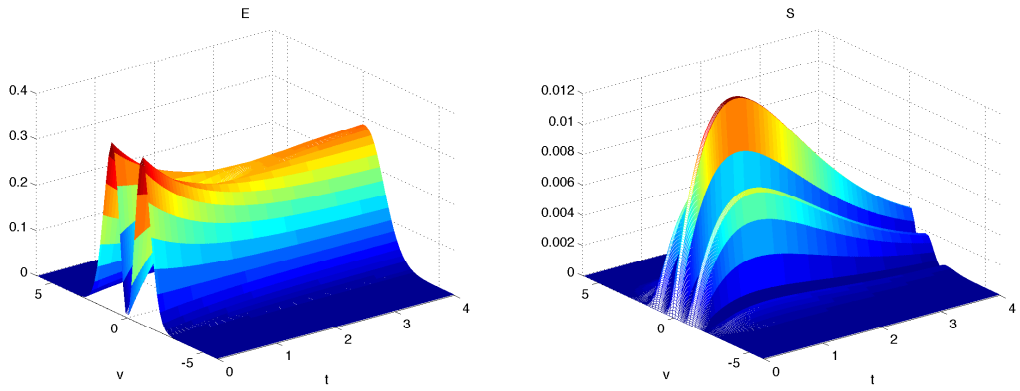

Figure 1: Example 1. Left: $\mathbb{E}[f](t,v)$. Right: $S[f](t,v)$. $K=7$, $N_v=64$, $\Delta t = 0.2/32$, RK-4 for time discretization.

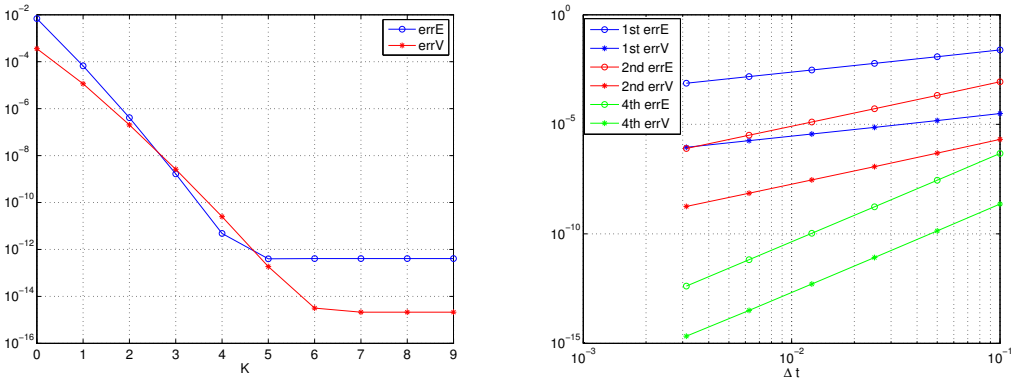

Figure 2: Example 1. Left: spectral accuracy in K ($\Delta t = 0.2/64$, RK-4 for time discretization). Right: 1st, 2nd, and 4th order accuracy in time ($K=9$). errE $= \|\mathbb{E}[f] - \mathbb{E}[f^{\text{ext}}]\|_{l^1(t,v)}$, errV $= \|\text{Var}[f] - \text{Var}[f^{\text{ext}}]\|_{l^1(t,v)}$.

and the initial data

$$f^0(\mathbf{v}) = \frac{1}{2\pi^2}\mathbf{v}^2 e^{-\mathbf{v}^2}.$$

Figure 3 shows the mean and standard deviation of f at $t = 2.5$ obtained using gPC up to 7th degree. The second-order Heun's method is applied for time discretization. The velocity space is discretized on 64×64 mesh, and $N_\sigma = 8$ for angular discretization.

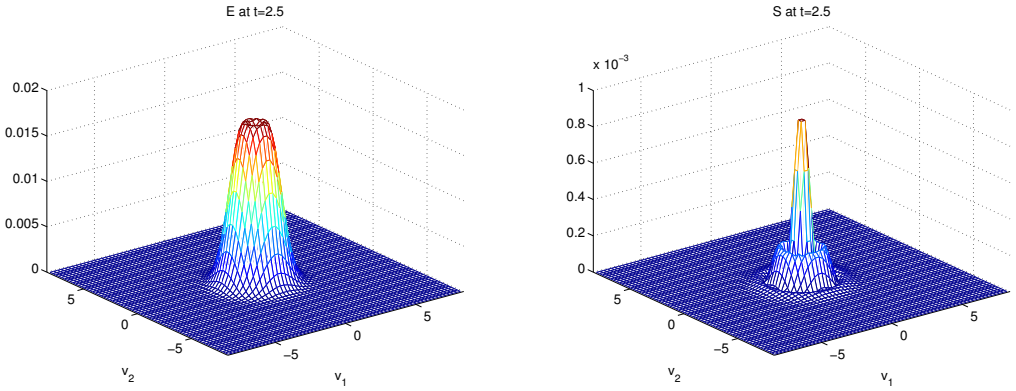

Figure 3: Example 2. Left: $\mathbb{E}[f](t = 2.5, \mathbf{v})$. Right: $S[f](t = 2.5, \mathbf{v})$. $K = 7$, $N_\mathbf{v} = 64$, $N_\sigma = 8$, $\Delta t = 0.1$, Heun for time discretization.

Without uncertainty, this is a famous benchmark example for the Boltzmann equation where the exact solution can be constructed [9]. However, it is not the case with a random collision kernel. We therefore compare our solution with the stochastic collocation [27] using 20 Gauss-Legendre quadrature points. The solutions at different time are plotted in Figure 4.

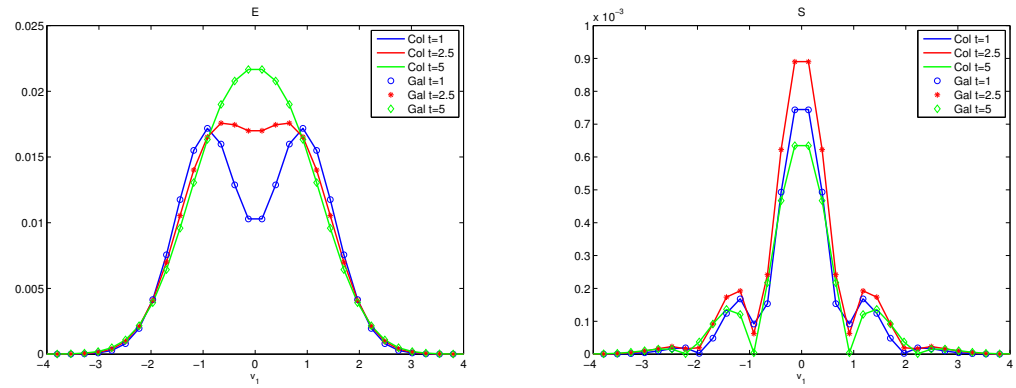

Figure 4: Example 2. $\mathbb{E}[f]$ and $S[f]$ at $v_2 = 0$. "Col" stands for collocation, "Gal" stands for Galerkin. Heun is used for Galerkin, RK-4 is used for collocation.

4.2.2 Random initial data

Example 3. Assume constant kernel $B = 1$ but random initial data

$$f^0(\mathbf{v}, z) = \frac{1}{2\pi^2}\mathbf{v}^2 e^{-\frac{\mathbf{v}^2}{1+sz}}, \quad s = 0.2,$$

we perform the same test as above. The results are shown in Figures 5 and 6. We see that the mean of the solution is more or less the same no matter whether the uncertainty is in collision kernel or initial data, whereas the standard deviation exhibits quite different behavior in the two cases.

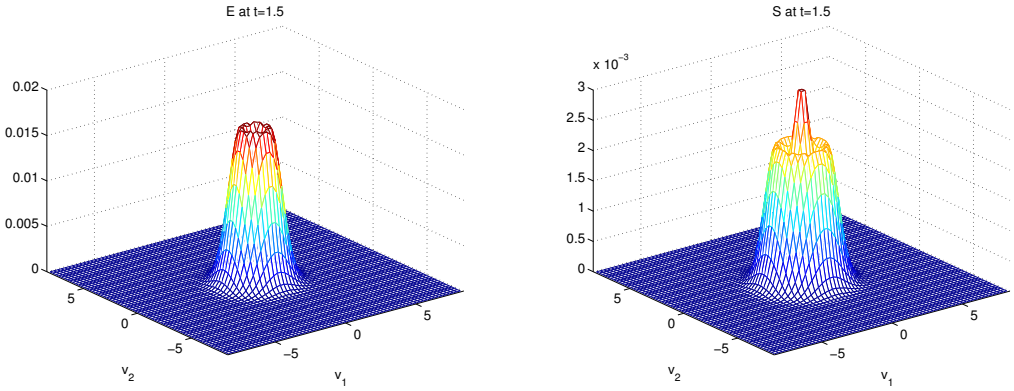

Figure 5: Example 3. Left: $\mathbb{E}[f](t = 1.5, \mathbf{v})$. Right: $S[f](t = 1.5, \mathbf{v})$. $K = 7$, $N_{\mathbf{v}} = 64$, $N_\sigma = 8$, $\Delta t = 0.1$, Heun for time discretization.

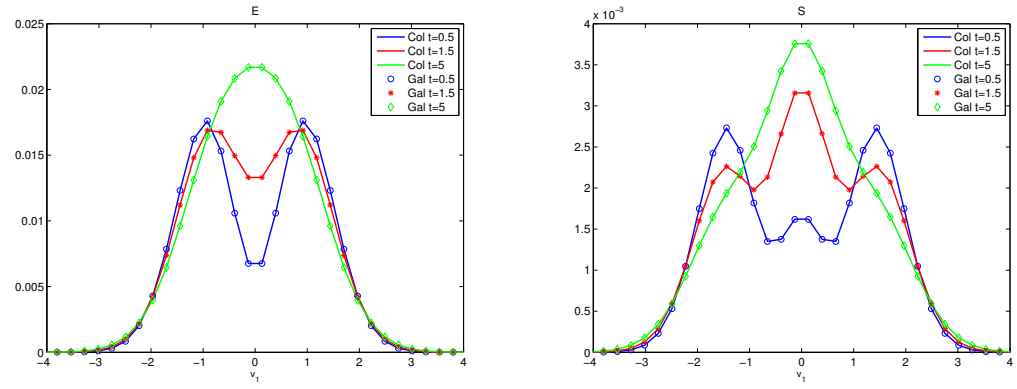

Figure 6: Example 3. $\mathbb{E}[f]$ and $S[f]$ at $v_2 = 0$. "Col" stands for collocation, "Gal" stands for Galerkin. Heun is used for Galerkin, RK-4 is used for collocation.

4.3 The spatially inhomogeneous Boltzmann equation

We finally consider the full Boltzmann equation and assume 1D in $\mathbf{x}$. For not too small Knudsen number Kn, time step Δt is mainly controlled by the CFL condition from the convection

part. In the following examples, we take a fixed CFL number 0.8 and implement the MUSCL scheme with minmod slope limiter for spatial discretization.

4.3.1 Random collision kernel

Example 4. Assume the collision kernel

$$B(z) = 1 + sz, \quad s = 0.6,$$

the continuous initial data

$$f^0(x, \mathbf{v}) = \frac{\rho^0(x)}{4\pi T^0(x)} \left(e^{-\frac{|\mathbf{v}-\mathbf{u}^0(x)|^2}{2T^0(x)}} + e^{-\frac{|\mathbf{v}+\mathbf{u}^0(x)|^2}{2T^0(x)}} \right), \quad x \in [0, 1], \tag{4.1}$$

where

$$\rho^0(x) = \frac{2 + \sin(2\pi x)}{3}, \quad \mathbf{u}^0 = (0.2, 0), \quad T^0 = \frac{3 + \cos(2\pi x)}{4}, \tag{4.2}$$

periodic boundary condition in x, and $\mathrm{Kn} = 0.1$. We compare the solution obtained by stochastic Galerkin with that of stochastic collocation on a finer mesh using 20 Gauss-Legendre quadrature points. The macroscopic quantities density, bulk velocity and temperature are depicted in Figure 7, where we observe good agreement between two methods.

4.3.2 Random initial data

In this subsection, we assume the randomness is only in initial data.

Example 5 (Shock tube problem).

Consider the equilibrium initial condition with random macroscopic quantities:

$$\begin{cases} \rho_l = 1 + s_1 \left(\dfrac{z+1}{2} \right), \quad u_l = 0, \quad T_l = 1 + s_2 z, \quad x \le 0.5, \\ \rho_r = 0.125, \quad u_r = 0, \quad T_r = 0.25, \quad x > 0.5. \end{cases}$$

To illustrate the effects of uncertainty in different macroscopic quantities, we examine two cases (1) $s_1 = 0.2$, $s_2 = 0$; (2) $s_1 = 0.2$, $s_2 = 0.1$. The results are shown, respectively, in Figures 8 and 9. The wiggles in the solution are due to the fact that a global gPC is used to approximate a discontinuous function, and can be improved by using local adaptive basis such as [26, 20].

Example 6. Consider the same initial data as in (4.1), (4.2) except

$$\rho^0(x, \mathbf{z}) = \frac{2 + \sin(2\pi x) + \frac{1}{2}\sin(4\pi x) z_1 + \frac{1}{3}\sin(6\pi x) z_2}{3},$$
$$T^0(x, \mathbf{z}) = \frac{3 + \cos(2\pi x) + \frac{1}{2}\cos(4\pi x) z_1 + \frac{1}{3}\cos(6\pi x) z_2}{4}.$$

These are chosen to mimic the K-L expansion. Periodic boundary condition is assumed in x. In the stochastic collocation, 10 Gauss-Legendre quadrature points are used for each random dimension. See results in Figure 10.

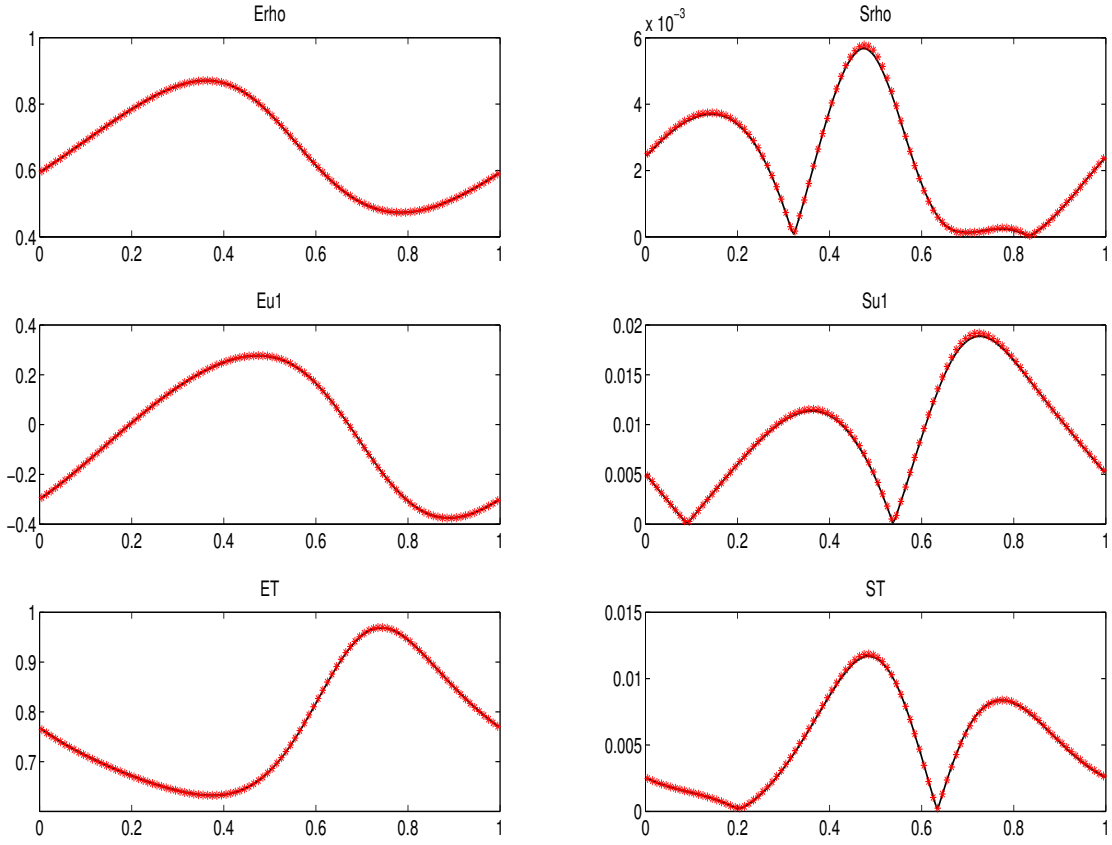

Figure 7: Example 4. Solutions at $t = 0.2$. Left column: mean of density, bulk velocity (first component), and temperature. Right column: standard deviation of density, bulk velocity (first component), and temperature. Solid line: collocation with $N_z = 20$, $N_{\mathbf{v}} = 64$, $N_\sigma = 8$, $N_x = 200$. Red star: Galerkin with $K = 7$, $N_{\mathbf{v}} = 32$, $N_\sigma = 4$, $N_x = 100$.

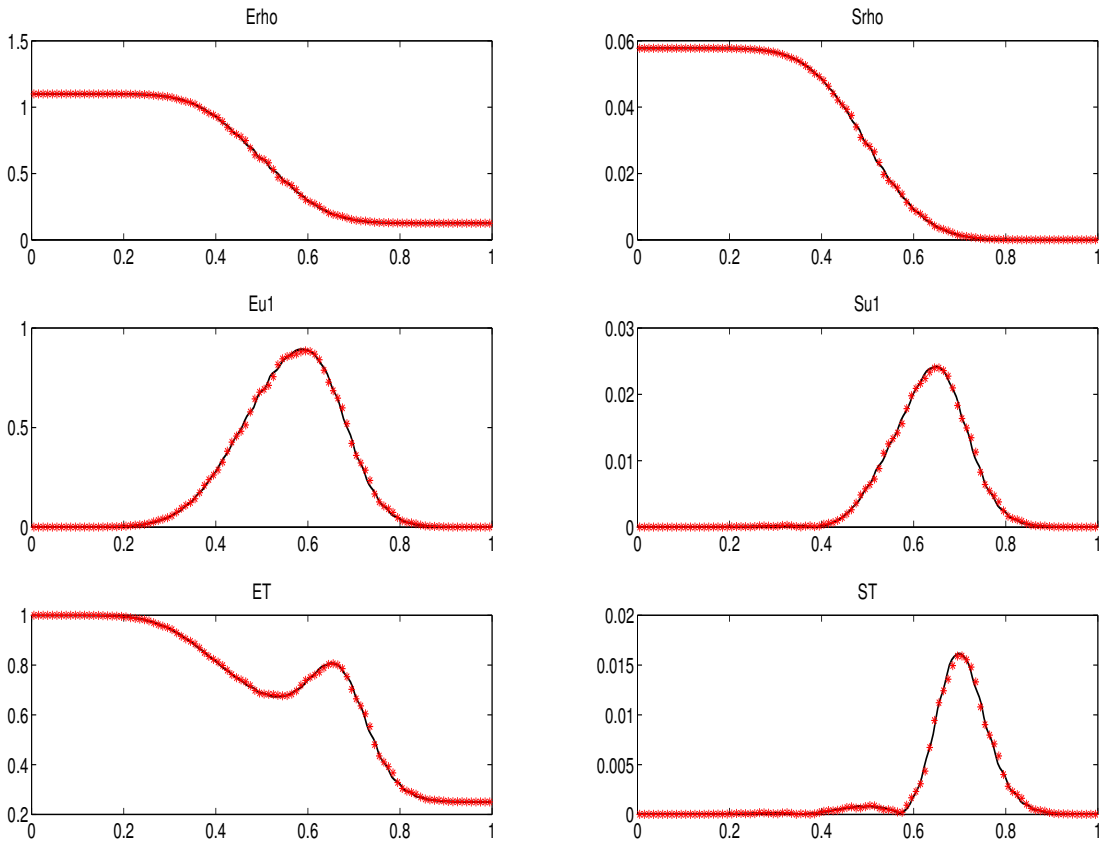

Figure 8: Example 5: case (1) $s_1 = 0.2$, $s_2 = 0$. Solutions at $t = 0.1$. Left column: mean of density, bulk velocity (first component), and temperature. Right column: standard deviation of density, bulk velocity (first component), and temperature. Solid line: collocation with $N_z = 20$, $N_{\mathbf{v}} = 64$, $N_\sigma = 8$, $N_x = 200$. Red star: Galerkin with $K = 7$, $N_{\mathbf{v}} = 32$, $N_\sigma = 4$, $N_x = 100$.

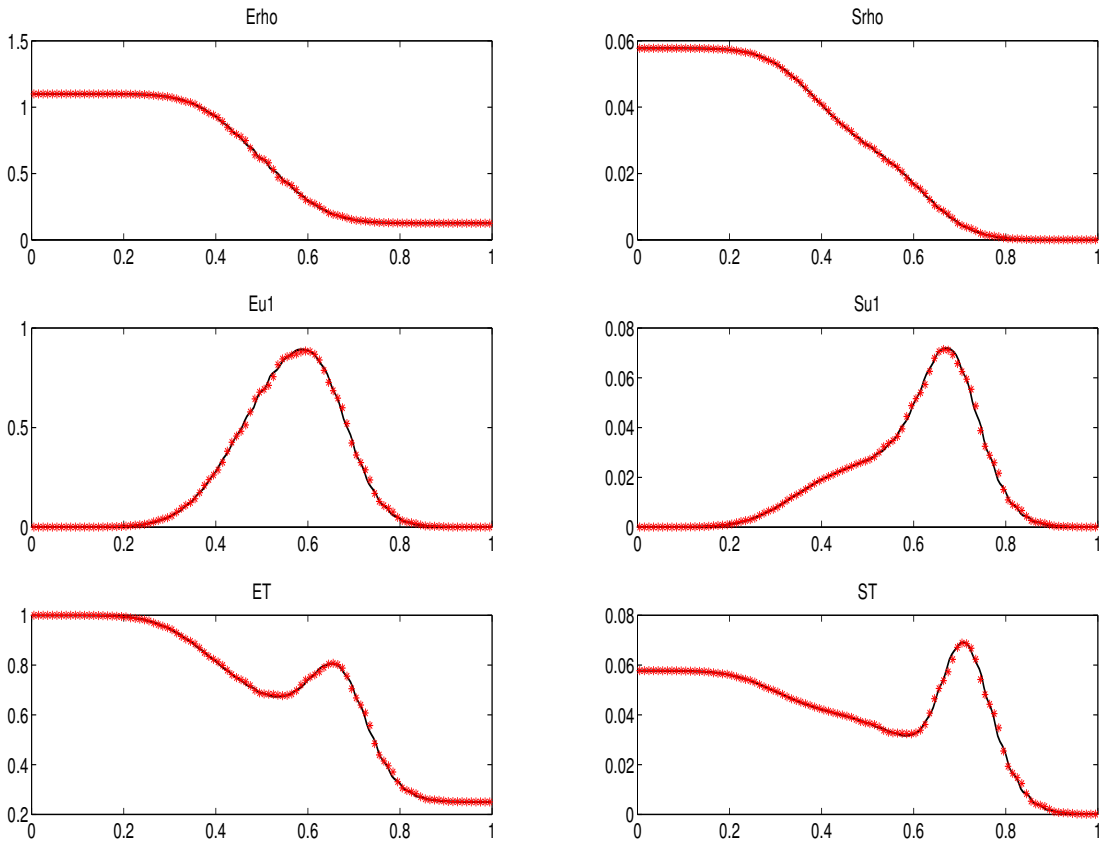

Figure 9: Example 5: case (2) $s_1 = 0.2$, $s_2 = 0.1$. Solutions at $t = 0.1$. Left column: mean of density, bulk velocity (first component), and temperature. Right column: standard deviation of density, bulk velocity (first component), and temperature. Solid line: collocation with $N_z = 20$, $N_{\mathbf{v}} = 64$, $N_\sigma = 8$, $N_x = 200$. Red star: Galerkin with $K = 7$, $N_{\mathbf{v}} = 32$, $N_\sigma = 4$, $N_x = 100$.

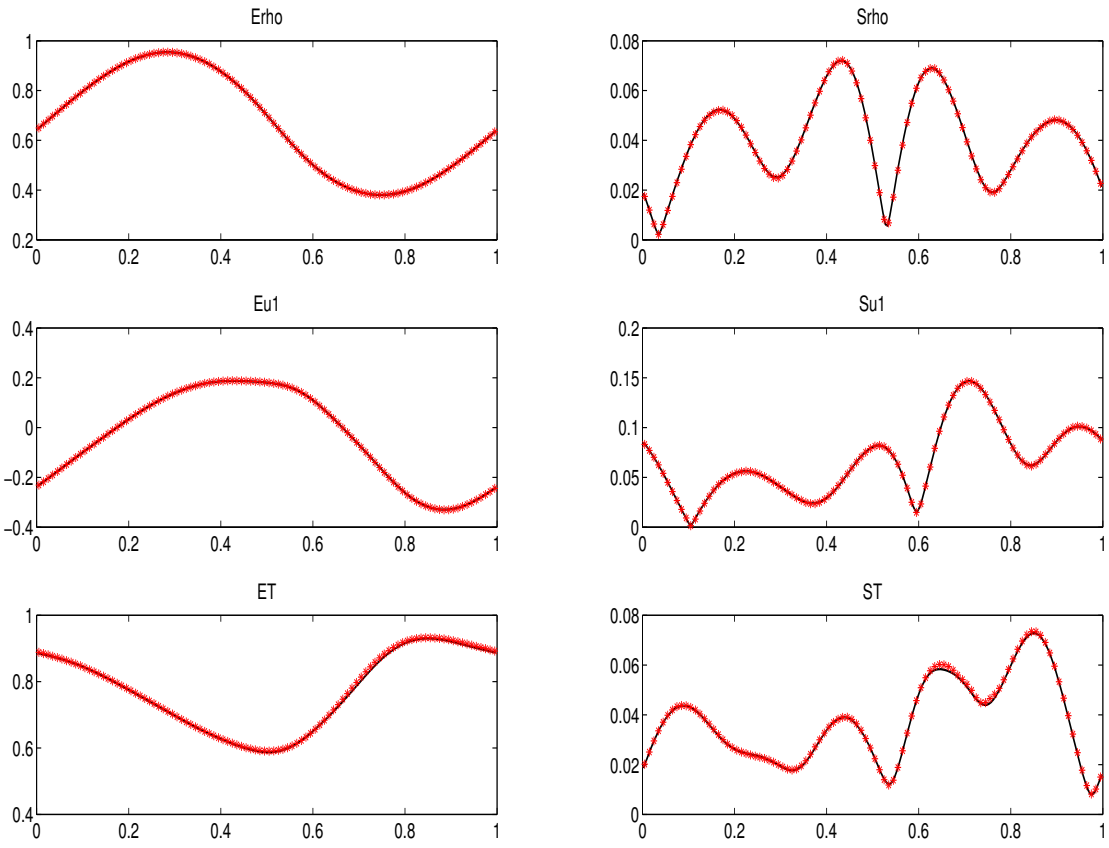

Figure 10: Example 6. Solutions at $t = 0.1$. Left column: mean of density, bulk velocity (first component), and temperature. Right column: standard deviation of density, bulk velocity (first component), and temperature. Solid line: collocation with $N_{\mathbf{z}} = 10$, $N_{\mathbf{v}} = 64$, $N_\sigma = 8$, $N_x = 200$. Red star: Galerkin with $K = 5$, $N_{\mathbf{v}} = 32$, $N_\sigma = 4$, $N_x = 100$.

4.3.3 Random boundary data

Example 7 (Sudden heating problem).

The gas is initially in a constant state

$$f^0(x,\mathbf{v}) = \frac{1}{2\pi T^0} e^{-\frac{\mathbf{v}^2}{2T^0}}, \quad T^0 = 1, \quad x \in [0,1].$$

At time $t = 0$, suddenly change the wall temperature at left boundary to

$$T_w(z) = 2(T_0 + sz), \quad s = 0.2.$$

Assume purely diffusive Maxwell boundary condition at $x = 0$, and $\mathrm{Kn} = 0.1$.

The deterministic version of this problem has been considered by many authors [1, 12, 10], where they all observed that with the sudden rise of wall temperature, the gas close to the wall is heated and accordingly the pressure there rises sharply, which pushes the gas away from the wall and a shock wave propagates into the domain. The mean of our solution also exhibits the similar behavior (see Figure 11). Meanwhile, the standard deviation of the solution allows us to predict the propagation of uncertainties quantitatively.

5 Conclusion

We have introduced a gPC based stochastic Galerkin scheme for the nonlinear Boltzmann equation with random inputs. For the first time, we are able to quantify the uncertainties coming from collision kernel, initial data, or boundary data. Along the way, we proposed a fast algorithm to accelerate the computation of collision operator in the gPC expansion. This paper serves as an initial attempt to UQ for nonlinear kinetic equations. Many interesting problems are open or currently under investigation, such as dimension reduction for high dimensional random input, asymptotic-preserving schemes that are efficient near the fluid dynamic regime, etc.

6 Appendix: fast Fourier-spectral method for the collision operator $\mathcal{Q}(g,h)$

In this appendix, we outline the fast Fourier-spectral method for computing the collision operator (3.7). First it suffices to consider an operator of the form

$$\mathcal{Q}(g,h)(\mathbf{v}) = \int_{\mathbb{R}^d}\int_{S^{d-1}} |\mathbf{v}-\mathbf{v}_*|^\lambda \left[g(\mathbf{v}')h(\mathbf{v}'_*) - g(\mathbf{v})h(\mathbf{v}_*)\right] \mathrm{d}\sigma \mathrm{d}\mathbf{v}_*,$$

where g and h are arbitrary functions of $\mathbf{v}$ (not necessarily positive). The starting point in [22] is to transform the above integral into a Carleman-like representation:

$$\mathcal{Q}(g,h)(\mathbf{v}) = \int_{\mathbb{R}^d}\int_{\mathbb{R}^d} \tilde{B}(\mathbf{x},\mathbf{y})\,\delta(\mathbf{x}\cdot\mathbf{y})\left[g(\mathbf{v}')h(\mathbf{v}'_*) - g(\mathbf{v})h(\mathbf{v}_*)\right] \mathrm{d}\mathbf{x}\,\mathrm{d}\mathbf{y}, \tag{6.1}$$

where $\mathbf{v}_* = \mathbf{v}+\mathbf{x}+\mathbf{y}$, $\mathbf{v}' = \mathbf{v}+\mathbf{x}$, $\mathbf{v}'_* = \mathbf{v}+\mathbf{y}$, and $\tilde{B}(\mathbf{x},\mathbf{y}) = 2^{d-1}|\mathbf{x}+\mathbf{y}|^{\lambda+2-d}$, so for 2D Maxwell molecule ($d = 2$, $\lambda = 0$) and 3D hard sphere molecule ($d = 3$, $\lambda = 1$), one has $\tilde{B} \equiv C$. The construction of Fourier spectral method for (6.1) can then be summarized as follows (assume $\tilde{B} = 1$):

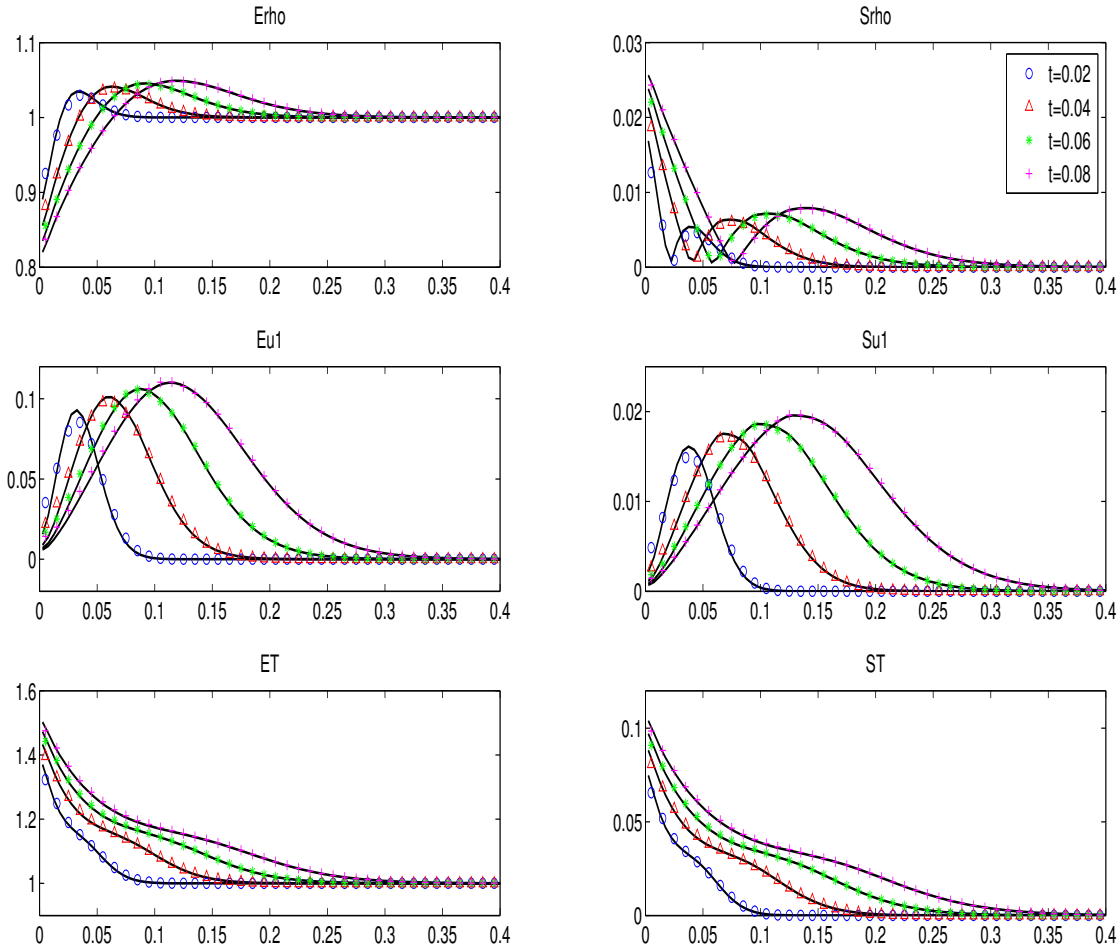

Figure 11: Example 7. Left column: mean of density, bulk velocity (first component), and temperature. Right column: standard deviation of density, bulk velocity (first component), and temperature. Solid line: collocation with $N_z = 20$, $N_{\mathbf{v}} = 64$, $N_\sigma = 8$, $N_x = 200$. Other legends are the Galerkin solutions at different time with $K = 7$, $N_{\mathbf{v}} = 32$, $N_\sigma = 4$, $N_x = 100$.

- Truncate the integral to a ball $\mathcal{B}_R$ (for both $\mathbf{x}$ and $\mathbf{y}$) with $R \geq 2S$, $\mathcal{B}_S \approx \mathrm{supp}_{\mathbf{v}}(g, h)$.
- Periodize g, h on the domain $\mathcal{D}_L = [-L, L]^d$. Choose $L \geq \frac{3\sqrt{2}+1}{2} S$ for anti-aliasing [23].
- Approximate g, h respectively by truncated Fourier series (note here k is a multi-dimensional index and is different from the main text):

$$g(\mathbf{v}) = \sum_k \hat{g}_k e^{i\frac{\pi}{L}k\cdot\mathbf{v}}, \quad h(\mathbf{v}) = \sum_k \hat{h}_k e^{i\frac{\pi}{L}k\cdot\mathbf{v}}, \quad k = -\frac{N_{\mathbf{v}}}{2}, \ldots, \frac{N_{\mathbf{v}}}{2} - 1. \tag{6.2}$$

- Substitute (6.2) into (6.1), and perform the standard Galerkin projection. The k-th mode of the Fourier expansion of $\mathcal{Q}$ is given by

$$\hat{\mathcal{Q}}_k = \sum_{l+m=k} \left[\beta(l, m) - \beta(m, m)\right] \hat{g}_l \hat{h}_m, \quad l, m, k = -\frac{N_{\mathbf{v}}}{2}, \ldots, \frac{N_{\mathbf{v}}}{2} - 1, \tag{6.3}$$

  with the kernel mode

$$\beta(l, m) = \int_{\mathcal{B}_R} \int_{\mathcal{B}_R} \delta(\mathbf{x} \cdot \mathbf{y}) e^{i\frac{\pi}{L}l\cdot\mathbf{x}} e^{i\frac{\pi}{L}m\cdot\mathbf{y}} \,\mathrm{d}\mathbf{x}\,\mathrm{d}\mathbf{y}. \tag{6.4}$$

It is clear that a direct computation of (6.3) (for all k) would require $O(N_{\mathbf{v}}^{2d})$ complexity. But if we can find a low-rank separated expansion of β as

$$\beta(l, m) \approx \sum_{r=1}^{M} A_r(l)\, B_r(m), \tag{6.5}$$

then the *weighted convolution* in (6.3) can be rendered into a *pure convolution*. Hence the cost will be reduced to $O(MN_{\mathbf{v}}^d \log N_{\mathbf{v}})$ by using the Fast Fourier Transform.

Now the question left is: how to find a decomposition as in (6.5)? We will explain the idea for 2D Maxwell molecule (readers are referred to [22] for other cases). In (6.4), expanding $\mathbf{x}$, $\mathbf{y}$ in polar coordinates, we have

$$\beta(l, m) = \frac{1}{4} \int_{S^1} \int_{S^1} \delta(\sigma_1 \cdot \sigma_2) \phi(l \cdot \sigma_1) \phi(m \cdot \sigma_2) \,\mathrm{d}\sigma_1 \mathrm{d}\sigma_2 = \int_0^{\pi} \phi(l \cdot \sigma_\theta) \phi(\sqrt{|m|^2 - (m \cdot \sigma_\theta)^2}) \,\mathrm{d}\theta, \tag{6.6}$$

where

$$\phi(s) := \int_{-R}^{R} e^{i\frac{\pi}{L}\rho s} \,\mathrm{d}\rho = 2R\,\mathrm{Sinc}\left(\frac{\pi}{L} R s\right), \quad \sigma_\theta := (\cos\theta, \sin\theta).$$

Note that the right hand side of (6.6) is a single integral in θ and the integrand is readily in decoupled form (also π-periodic in θ). Therefore, we can approximate β by a uniform quadrature rule:

$$\beta(l, m) \approx \left(\frac{\pi}{N_\sigma}\right) \sum_{r=1}^{N_\sigma} \phi(l \cdot \sigma_{\theta_r}) \phi(\sqrt{|m|^2 - (m \cdot \sigma_{\theta_r})^2}),$$

hence resulting in the desired form.

References

[1] K. Aoki, Y. Sone, K. Nishino, and H. Sugimoto. Numerical analysis of unsteady motion of a rarefied gas caused by sudden changes of wall temperature with special interest in the propagation of a discontinuity in the velocity distribution function. In A. E. Beylich, editor, *Rarefied Gas Dynamics*, pages 222–231, 1991.

[2] G. A. Bird. *Molecular Gas Dynamics and the Direct Simulation of Gas Flows*. Clarendon Press, Oxford, 1994.

[3] F. Bouchut and L. Desvillettes. A proof of the smoothing properties of the positive part of Boltzmann's kernel. *Rev. Mat. Iberoamericana*, 14:47–61, 1998.

[4] C. Cercignani. *The Boltzmann Equation and Its Applications*. Springer-Verlag, New York, 1988.

[5] C. Cercignani. *Rarefied Gas Dynamics: From Basic Concepts to Actual Calculations*. Cambridge University Press, Cambridge, 2000.

[6] C. Cercignani, R. Illner, and M. Pulvirenti. *The Mathematical Theory of Dilute Gases*. Springer-Verlag, 1994.

[7] S. Chapman and T. G. Cowling. *The Mathematical Theory of Non-Uniform Gases*. Cambridge University Press, Cambridge, third edition, 1991.

[8] G. Dimarco and L. Pareschi. Numerical methods for kinetic equations. *Acta Numer.*, 23:369–520, 2014.

[9] M. H. Ernst. Exact solutions of the nonlinear Boltzmann equation. *J. Stat. Phys.*, 34:1001–1017, 1984.

[10] F. Filbet. On deterministic approximation of the Boltzmann equation in a bounded domain. *Multiscale Model. Simul.*, 10:792–817, 2012.

[11] F. Filbet, C. Mouhot, and L. Pareschi. Solving the Boltzmann equation in NlogN. *SIAM J. Sci. Comput.*, 28:1029–1053, 2006.

[12] I. Gamba and S. H. Tharkabhushanam. Shock and boundary structure formation by spectral-Lagrangian methods for the inhomogeneous Boltzmann transport equation. *J. Comput. Math.*, 28:430–460, 2010.

[13] R. G. Ghanem and P. D. Spanos. *Stochastic Finite Elements: A Spectral Approach*. Springer-Verlag, New York, 1991.

[14] J. Hirschfelder, R. Bird, and E. Spotz. The transport properties for non-polar gases. *J. Chem. Phys.*, 16:968–981, 1948.

[15] S. Jin. Asymptotic preserving (AP) schemes for multiscale kinetic and hyperbolic equations: a review. *Riv. Mat. Univ. Parma*, 3:177–216, 2012.

[16] S. Jin, D. Xiu, and X. Zhu. Asymptotic-preserving methods for hyperbolic and transport equations with random inputs and diffusive scalings. *J. Comput. Phys.*, 289:35–52, 2015.

[17] K. Koura and H. Matsumoto. Variable soft sphere molecular model for inverse-power-law or Lennard-Jones potential. *Phys. Fluids A*, 3:2459–2465, 1991.

[18] M. Loève. *Probability Theory*. Springer-Verlag, New York, fourth edition, 1977.

[19] X. Lu. A direct method for the regularity of the gain term in the Boltzmann equation. *J. Math. Anal. Appl.*, 228:409–435, 1998.

[20] O. Le Maitre, O. Knio, H. Najm, and R. Ghanem. Uncertainty propagation using Wiener-Haar expansions. *J. Comput. Phys.*, 197:28–57, 2004.

[21] O. P. Le Maitre and O. M. Knio. *Spectral Methods for Uncertainty Quantification: With Applications to Computational Fluid Dynamics*. Springer, 2010.

[22] C. Mouhot and L. Pareschi. Fast algorithms for computing the Boltzmann collision operator. *Math. Comp.*, 75:1833–1852, 2006.

[23] L. Pareschi and G. Russo. Numerical solution of the Boltzmann equation I: spectrally accurate approximation of the collision operator. *SIAM J. Numer. Anal.*, 37:1217–1245, 2000.

[24] B. van Leer. Towards the ultimate conservative difference scheme V. A second order sequel to Godunov's method. *J. Comput. Phys.*, 32:101–136, 1979.

[25] C. Villani. A review of mathematical topics in collisional kinetic theory. In S. Friedlander and D. Serre, editors, *Handbook of Mathematical Fluid Mechanics*, volume I, pages 71–305. North-Holland, 2002.

[26] X. Wan and G. E. Karniadakis. An adaptive multi-element generalized polynomial chaos method for stochastic differential equations. *J. Comput. Phys.*, 209:617–642, 2005.

[27] D. Xiu. *Numerical Methods for Stochastic Computations*. Princeton University Press, New Jersey, 2010.